Thermostructural and Material Considerations in the Design of the F-14 Aircraft Transparencies

S. Z. Fixler*
Grumman Aerospace Corporation, Bethpage, N.Y.

The evolution of the design is traced, along with in-service-dictated modifications, under the constraints of cost, weight, and schedule without sacrificing vital performance. Design requirements are given, along with the systems that affect the load and thermal environments. Tradeoffs between monolithic and multilaminate configurations are shown. Windshield and canopy temperature, thermal stress distributions, and distortions are presented. Transparency material ranking criteria are given. Predicted and in-flight measured canopy temperature correlations are shown. It is shown how various factors influenced the decision processes in arriving at a successful design.

Introduction

THE problem was to design, develop, and test a transparent cockpit enclosure for the F-14 aircraft that would combine high strength, light weight, maximum visibility, and minimum distortion within the entire flight envelope under all operating conditions. This paper presents the thermostructural and material aspects of the solution to that problem. The evolution of the transparency final design is traced, along with in-service-dictated modifications, through the various stages from the proposal through fleet deployment. Design concepts are described, and results of thermostructural analyses and tests are presented.

Extremes in the operational and environmental conditions of the high-performance F-14 fighter have posed a host of problems to the transparency engineering and design teams. The problem faced on the F-14 was how best to meet tomorrow's challenge with yesterday's experience and today's capabilities. One of the more challenging tasks was to strike a proper balance between the functions to be performed by the transparencies and the constraints imposed by extraneous boundary conditions. Vital transparency performance was to be maximized under the constraints of mission severity, cost, weight, desired reliability, and schedule.

Crucial decisions affecting overall design concepts had to be made early in the program because of abbreviated schedules. A decision that contributed significantly to the eventual success of the program was one concerning material selection. A decision had to be made whether to proceed with a conservative but highly reliable design, using an acrylic canopy and a flat glass windshield; or to proceed with a contoured windshield and a class of glamour materials whose claimed performance was not established experimentally. The decision was made to go conservative.

Overall System Description

The F-14 cockpit is enclosed by a flat, multilaminate glass/polyvinyl butyral (PVB) front windshield; two double-curvature, trilaminate acrylic side windshields; and by a one-piece, clamshell, rear-hinged canopy. The canopy is comprised of two double-curvature trilaminate acrylic panels in an aluminum frame. The entire transparent enclosure is shown and described in Fig. 1.

Ancillary cockpit systems that affect the loads and thermal environment of the transparent enclosure include the cockpit pressurization system, cockpit environmental-control system, windshield anti-ice system, windshield rain-removal system, windshield and canopy-defog system, and the canopy-jettison system. The pertinent system parameters that affect the transparency load and temperature environments are listed in Table 1.

Design Requirements

Front Windshield

The F-14 front windshield is a multifunction device. It provides undistorted vision for the pilot, acts as a bullet (and bird) resistant shield, and displays vital flight control and weapon system information to the pilot. The last function, namely, direct Head-Up Display (HUD) windshield projection, is an F-14 first, and has proven to be very effective in service. A full discussion on the F-14 HUD is given in Ref. 1. What is relevant from a structural point of view is the following: Direct HUD windshield projection was an in-service-dictated modification that resulted in an increased windshield weight and material change. Due to flatness requirements, the inner windshield ply was changed from semitempered glass to annealed glass. Due to optical and geometric considerations, the windshield thickness was increased from approximately 1.26 in. to approximately 1.85 in. The change from semitempered glass to annealed glass decreased the thermal shock resistance of the windshield (see the discussion on materials).

The front windshield is a flat multilaminate glass/PVB composite shown in cross section in Fig. 2. It also shows the edge attachment, method of mounting, and the frame cross

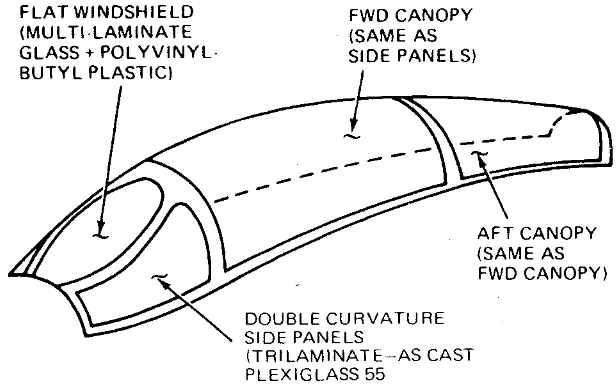

Fig. 1 F-14 transparent cockpit enclosure.

Presented as Paper 75-990 at the AIAA 1975 Aircraft Systems and Technology Meeting, Los Angeles, Calif., Aug. 4-7, 1975; submitted Sept. 11, 1975; revision received Aug. 25, 1976.

Index categories: Aircraft Structural Design (including Loads); Thermal Stresses.

*Structural Mechanics Group Leader. Member AIAA.

Table 1 Cockpit ancillary system parameters

Cockpit ancillary system	Type	Max. temperature and/or pressure	Affected transparency
Anti-ice	hot air blast	390°F	front windshield exterior surface
Rain removal and rain repellent	hot air blast and chemical spray	390°F 22 psi	front windshield exterior surface
Defog	initially elect. heating elements, subsequently hot air blast	350°F	front windshield inner surface
Environmental control	engine bleed air	60°F to 80°F	inner surface of all transparencies
Cockpit pressurization	—	5 psig	all
Jettison	—	—	forward and rear canopies

Table 2 Front windshield

Thermostructural design requirements	
Bird impact	4-lb bird at 350 knots
Projectile impact	required by spec: 1-¼ in.-thick bullet-resistant glass good for: Cal. 0.50 @71° obliquity, or for Cal. 0.30 @32° obliquity
Internal pressure	11.4 psi ultimate
Aerodynamic load	triangular distribution of 18 psi at front decreasing to zero at bow
Fatigue pressure	5.7 psi, 24,000 cycles
Thermal load	aerodynamic heating, anti-icing, rain dispersing, and defogging (see Table 1)
Underwater implosion load	15 ft of water

section. The windshield was designed to withstand internal pressurization, external aerodynamic load, thermal load, bird impact, and projectile impact. The design requirements for the front windshield are listed in Table 2. Most of the structure was designed by bird impact using the bird bouncing technique. In bird bouncing, as opposed to bird catching, the glass is the dominant factor in absorbing the impact load requiring thinner PVB interlayers. The F-4 and A-7 windshields are based on the same concept. Detailed F-14 windshield stress analysis is reported in Ref. 2.

Figure 3 shows a correlation of recent bird impact test data reported in Ref. 3. The test specimens were constructed with thin PVB interlayers in conformity with the bird-bouncing technique. The curve gives the bird impact velocity that will fail a given-thickness windshield. The solid lines are test data for thermally toughened glass. The dashed lines give the windshield failing speeds if, in addition to the thermally toughened glass, the energy absorption of the annealed glass is included. It is seen that for a 4-lb bird the F-14 design is good for velocities of over 400 knots.

Canopy and Side Windshields

The forward and rear canopies are double curvature 0.4-in. thick trilaminates consisting of a 0.1-in.-thick outer layer of as-cast Plexiglass-55, a 0.1-in.-thick cast-in-place (CIP) interlayer, and a 0.205-in.-thick inner load-carrying member of 75% stretched arcylic. An exploded view of a canopy cross section showing the attachment method, material identification, and frame is presented in Fig. 4. The side windshields were analyzed as a 0.525-in.-thick trilaminate consisting of a 0.125-in.-thick outer layer of as-cast Plexiglass-55, a 0.1-in.-thick CIP interlayer, and a 0.3-in.-thick inner load-carrying laminate of 75% stretched acrylic. The method of attachment is similar to that of the canopy as shown in Fig. 2.

The canopies and side windshields were designed to withstand internal pressurization, external aerodynamic load,

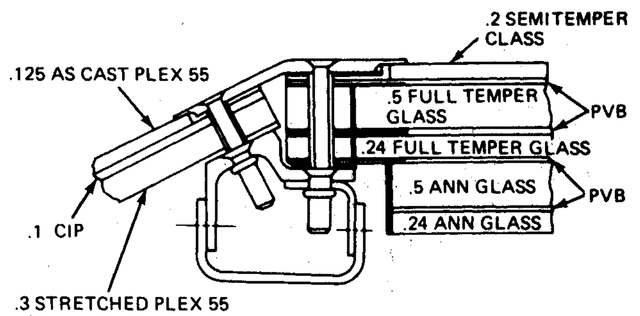

Fig. 2 Cross section through front and side windshields.

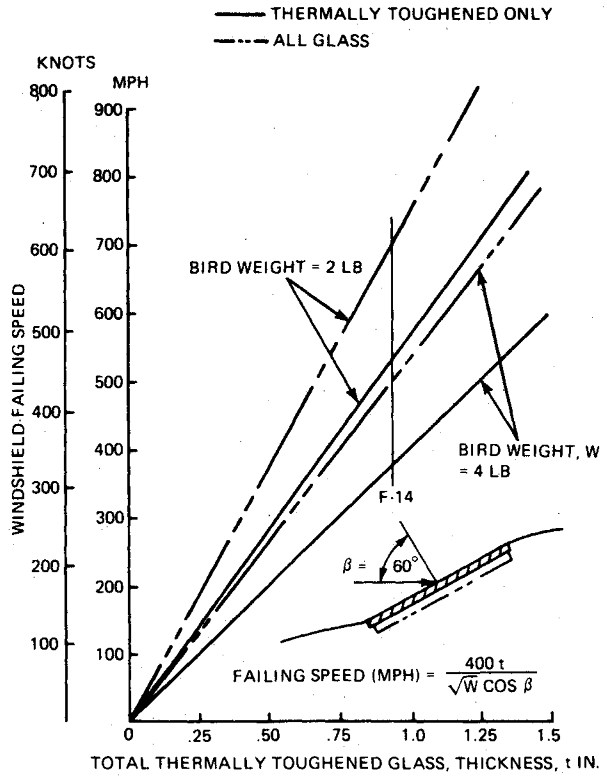

Fig. 3 Correlation of recently reported bird impact test data.

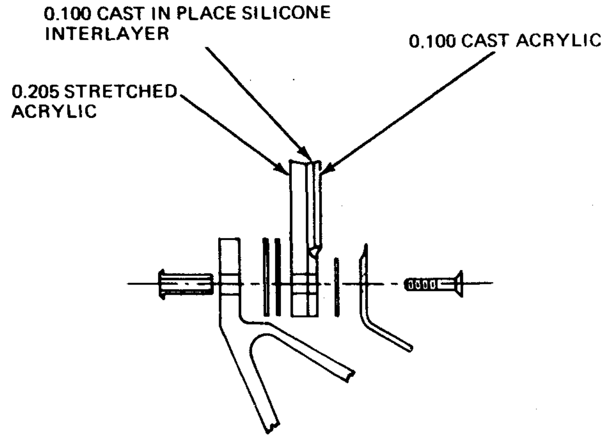

Fig. 4 Exploded view of canopy cross section.

Table 3 Canopy and side windshields

Thermostructural design requirements	
Internal pressurization	11.4 psi ultimate
Fatigue pressure	5.7 psi, 24,000 cycles
Aerodynamic load	side windshields: triangular distribution of 18 psi at front, decreasing to zero at bow. canopy: 3.27 psi ultimate
Thermal load	aerodynamic heating, internal heating
Under water implosion load	15 ft of water
Canopy jettison	600 knots EAS max.

jettison loads (canopy only), thermal loads, and underwater implosion loads. The design requirements for the side windshields and canopy are listed in Table 3.

Material Considerations

Materials are the key to a successful aircraft transparency design. In the F-14 design, materials played their proper role. A decision had to be made early in the program whether to proceed with a class of materials having modest but time-tested performance, or to yield to the temptation of furthering the state-of-the-art and proceed with transparencies showing great promise in selected material property categories, but which had no proven record of performance in the field. The first class was represented by the acrylics and soda lime glasses and the second by polycarbonates, acrylic-polycarbonates, and by specially formulated glass compositions. The decision was made to design the F-14 transparency with the less glamorous, but highly reliable and less costly acrylic/soda lime glass system. The successful transparency design that subsequently evolved stemmed, to a great extent, from that decision.

In considering transparent material candidates, thermal shock resistance is one of the more important parameters. Following Przemieniecki,[4] a thermal shock resistance index (TSRI) can be defined as $TSRI = \alpha' S(1-\nu)/\alpha E$ where α' = thermal diffusivity, ft^2/hr; S = tensile strength (or modulus of rupture), psi; ν = Poisson's ratio; E = Young's modulus, psi; α = coefficient of thermal expansion, in./in.-°F.

The material with a higher TSRI value will generally have better thermal and strength characteristics. Several windshield glass candidates were evaluated using the TSRI as a material ranking criterion. Figure 5 shows the ranking of various glasses considered for the F-14 front windshield. The strong effect of temper and formulation on thermal shock resistance is evident. It is also evident that the choice of soda lime glass for the F-14 front windshield was not based on thermal shock

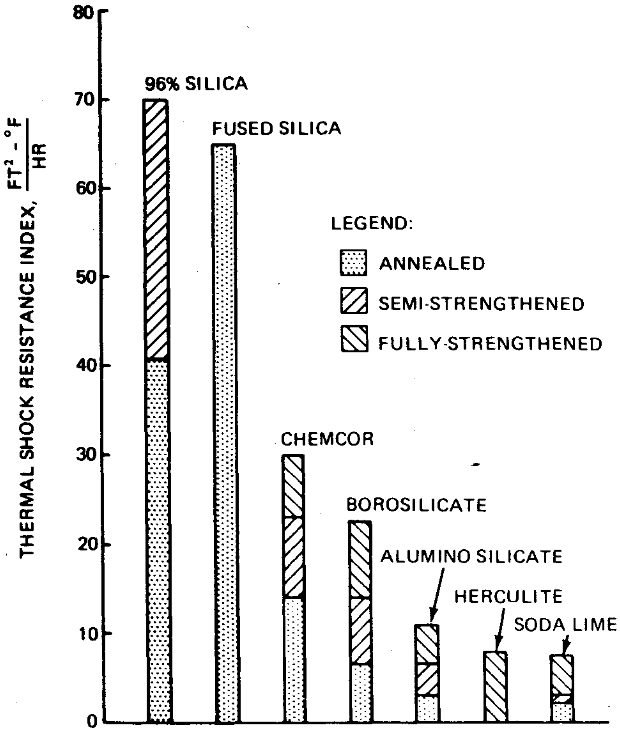

Fig. 5 Windshield material ranking: resistance to thermal shock.

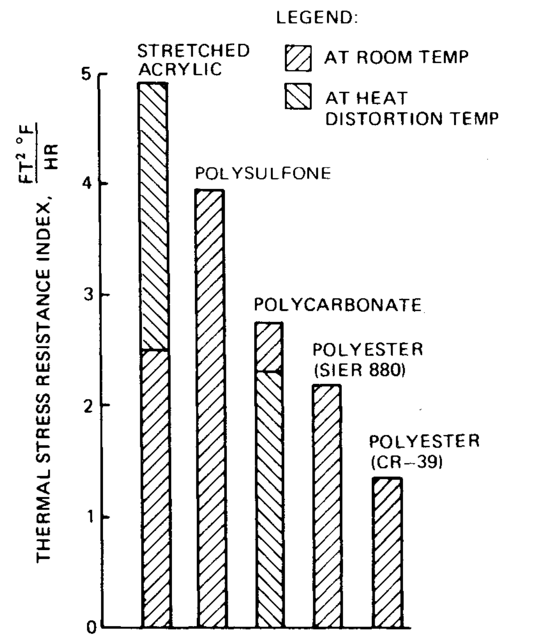

Fig. 6 Canopy material ranking: resistance to thermal stress.

resistance considerations alone. Other criteria, such as good optical properties, high abrasion resistance, low cost, and proven past performance have tipped the scale for soda lime glass of the F-14.

A similar TSRI material ranking was performed on several canopy materials as shown in Fig. 6. In the case of these materials, however, the TSRI has to be looked at as a resistance index to thermal stresses in general, not just thermal shock. This is true, as thermal stresses are generally proportional to $\alpha E \Delta T/(1-\nu)$, and a high diffusivity (α') tends to reduce the ΔT. It therefore follows that the product of α' and $(1-\nu)/\alpha E$ is a measure of the resistance to thermal stress.

Because the TSRI is temperature sensitive, it was evaluated at room temperature and at the heat-distortion temperature.

Table 4 Mission profiles used in study

Mission no.	Altitude, ft	Steady-state Mach no.	Max Mach no.	Duration at steady-state Mach no., min	Duration at Max Mach no., min
1	35,000	1.8	specified	2.85	variable
2	35,000	2.0	specified	2.5	variable
3	35,000	2.2	specified	2.17	variable
4	34,000	2.2	steady-state	4.11	—
5	37,500	2.2	specified	—	variable

TSRI values at the heat distortion temperature are more meaningful, because it is at the high end of the temperature spectrum that canopies tend to fail. It should be noted that while polycarbonates have a higher TSRI value than stretched acrylics at room temperature, they have a considerably lower TSRI value (less than half) at the heat distortion temperature.

As in the case of the front windshield, the most significant factor that decided in favor of acrylics for the side windshields and canopy was a high level of confidence in its ultimate performance.

Canopy Tradeoff Studies

The question of a monolithic versus a trilaminate canopy became an important issue at the start of the program. The increases in weight, cost, and complexity, and the decrease in optical qualities associated with a trilaminate construction were enough reason to make every effort to save the monolithic concept. A monolithic stretched acrylic rear canopy was contained in the F-14 proposal. A tradeoff study was launched in order to arrive at feasible design alternatives that would not impose undue limitations on airplane performance or interfere with existing schedules or weight targets. The parameters that were varied in the analysis included mission profiles, structural configurations, and heat transfer coefficients. Five different mission profiles and ten different structural configurations were analysed at three levels of heat transfer.

The mission profiles are listed in Table 4. Missions Nos. 1 through 3 are deck-launched intercept missions consisting essentially of a maximum afterburning (A/B) climb to 35,000 ft, acceleration to a steady-state (nonthermal) Mach number (loiter), followed by a final dash at the maximum Mach number. These missions were constructed under the following constraints: a) a variable stay time at maximum Mach, b) a fuel-capacity-limited stay time at the steady-state Mach number; and c) a specified mission radius. In Mission No. 4, the dash portion was eliminated, and the combat altitude in Mission No. 5 was assumed at 37,500 ft. Only acrylics were considered in the analysis.

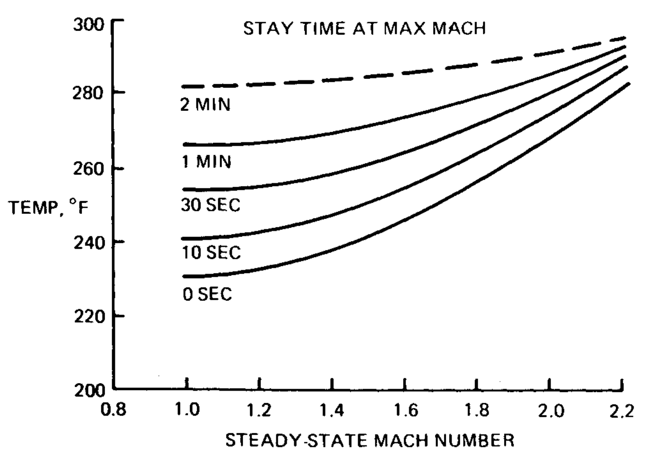

Fig. 7 Rear canopy surface temperature at maximum Mach after acceleration from steady-state Mach number.

Initially, an analysis was made to determine the maximum (thermal) steady-state Mach number that could be maintained prior to a maximum A/B acceleration to the maximum Mach number. In this case, the canopy was assumed to be thermally soaked at the steady-state Mach number. The results for a monolithic rear canopy are shown in Fig. 7 for different stay times at maximum Mach, 35,000 ft. As shown, stay times at maximum Mach greater than 20 sec cannot be preceded by a supersonic steady-state Mach number without exceeding an outer-surface temperature of 250°F on the rear canopy. By specification, stretched acrylics are not to exceed 250°F. These results were based on existing acceleration rates and nominal heat transfer coefficients.

In the next phase of the analysis, the stay-times at the (nonthermal) steady-state Mach numbers were limited by the aircraft fuel capacity. Figure 8 shows the maximum rear canopy surface temperature as a function of maximum Mach-stay-time and steady-state Mach number prior to maximum Mach for the various missions investigated. The results indicate that the temperature relief obtained by reducing the

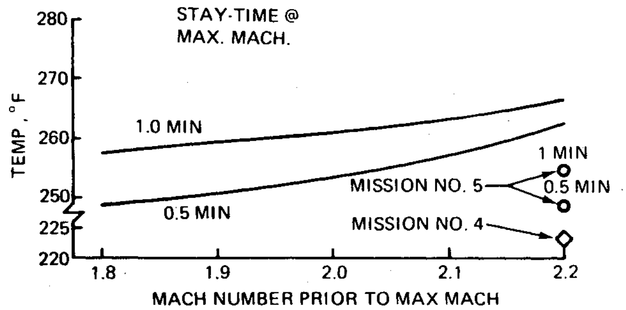

Fig. 8 Effect of mission profiles on monolithic canopy temperatures

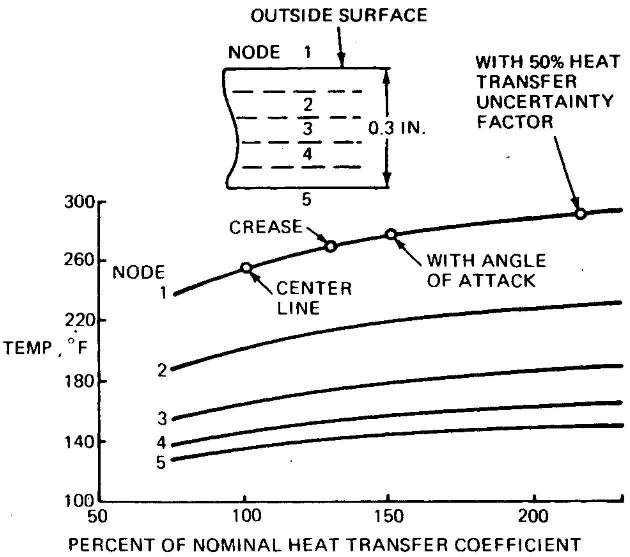

Fig. 9 Effect of heat transfer coefficient on monolithic cano temperatures.

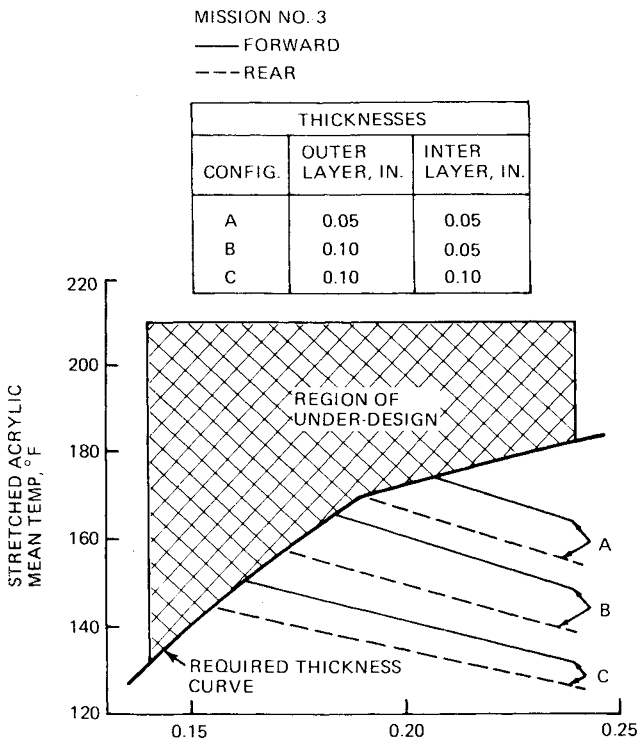

Fig. 10 Trilaminate canopy optimization.

prior (steady-state) Mach number from 2.2 (Mission 3) to 1.8 (Mission 1) does not warrant the resultant limitations on aircraft performance.

The effect of heat-transfer coefficient on the rear canopy temperature levels (maximum during mission) is shown in Fig. 9. The results are for Mission No. 5, but the trend may be taken as typical. The heat-transfer coefficients used in the analysis were taken from Ref. 5. The variation of outer-surface temperature from centerline to crease, and the effects of angle-of-attack and a 50% heat-transfer uncertainty factor on the outer-surface temperature are also shown. With a temperature distribution as shown (outside surface temperature equals 295°F), the structural integrity of the monolithic rear canopy became questionable and the concept was abandoned.

Figure 10 shows a plot of stretched acrylic mean temperature as a function of stretched acrylic thickness for three different trilaminate structural configurations. Superimposed on the plots is the required-thickness curve, which gives required thickness of stretched acrylic for a given mean temperature to satisfy strength criteria. The cross-hatched area represents a region where the canopy would have insufficient strength. The temperatures were based on crease-heat-transfer coefficients with no penalties for angle-of-attack or heat-transfer uncertainties.

Intersections of the required-thickness curve with temperature lines (A, B, and C in Fig. 10) give the required thicknesses of stretched acrylic for an optimized canopy with respect to strength and temperature. These thicknesses (when translated into weight) give the results shown in Fig. 11. The "lightest-possible" designation in Fig. 11 represents a temperature/strength optimized canopy without consideration of producibility, service degradation, or cost of manufacture. The "most-feasible" designation stands for what was thought to be within the realm of producibility. This was to be confirmed by the various canopy manufacturers.

As seen in Fig. 11, by going from a monolithic to a trilaminate rear canopy (most feasible) a 13-lb weight penalty is incurred. On the other hand, the lightest configuration has a potential weight saving of 13 lb. [Note that the final canopy

CONFIGURATION	THICKNESS, IN.					
	FORWARD			REAR		
	A/C	CIP	S/A	A/C	CIP	S/A
A	.10	.125	.205	.10	.125	.205
B	.10	.10	.25	–	–	.30
C	.10	.10	.20	.20	.10	.1875
D	.10	.10	.20	–	–	.30
E	.05	.05	.217	.05	.05	.20

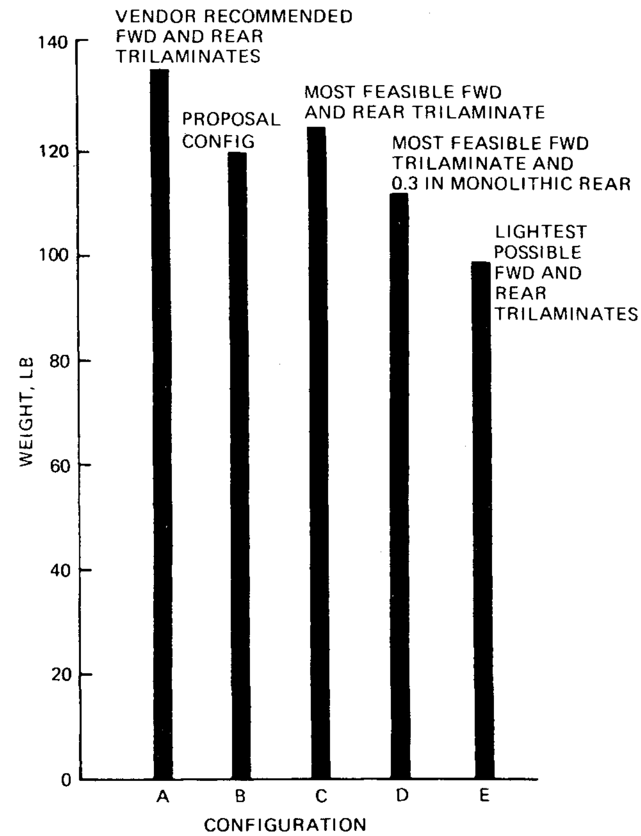

Fig. 11 Weights for canopy alternatives.

laminate thicknesses (Fig. 4) are rather close to those of the most feasible configuration shown in Fig. 11 (configuration C).]

Temperature Distribution

Windshield and canopy temperature distributions were computed using the latest computerized numerical techniques that allow for multidimensional, multimode heat transfer, as well as precise boundary conditions. The outer surface was subjected to radiation (including solar load) and to the convective boundary layer. The inner surface boundary conditions were taken as radiation and convection to a cockpit interior of 80°F. The canopy external heat-transfer coefficients and forcing functions were determined by an exact flowfield solution using the Grumman-Imbedded Shock Program as described in Ref. 6. Angle-of-attack effects were accounted for by two-dimensional wedge flow theory. Internal heat-transfer coefficients were computed by the basic Colburn equation, modified to fit the specific internal flow geometries.

The front windshield was analyzed as a composite (Fig. 2). Temperature distribution and response to the Basic Thermal Mission Profile† are shown in Fig. 12 along with the nodal

†The Basic Thermal Mission Profile represents the most severe thermal environment on most of the F-14 structure.

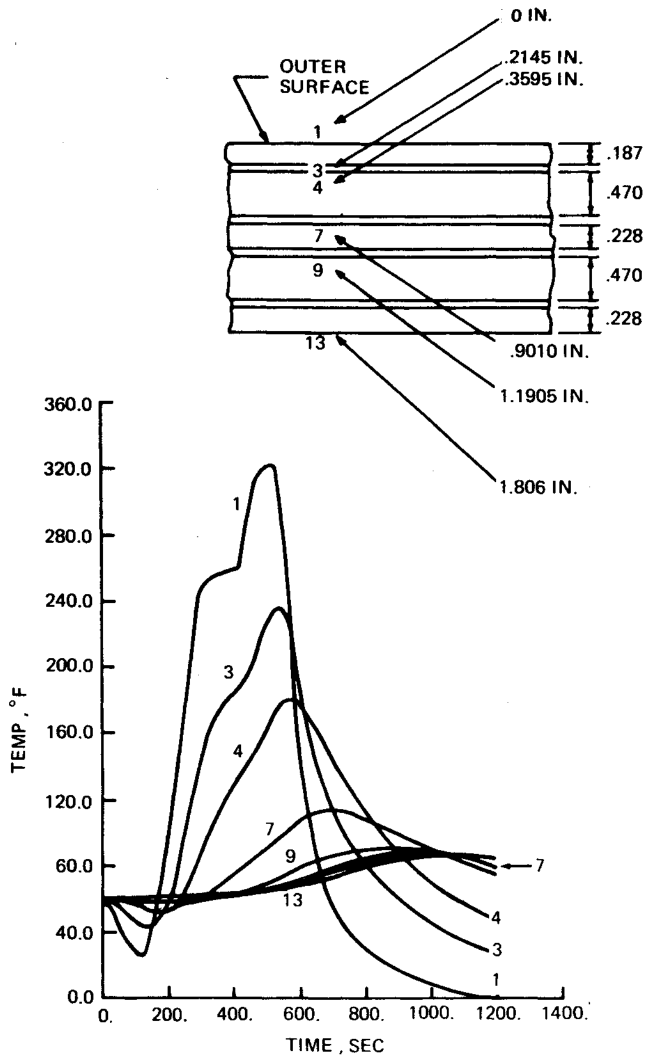

Fig. 12 Forward windshield thermal response to basic thermal mission.

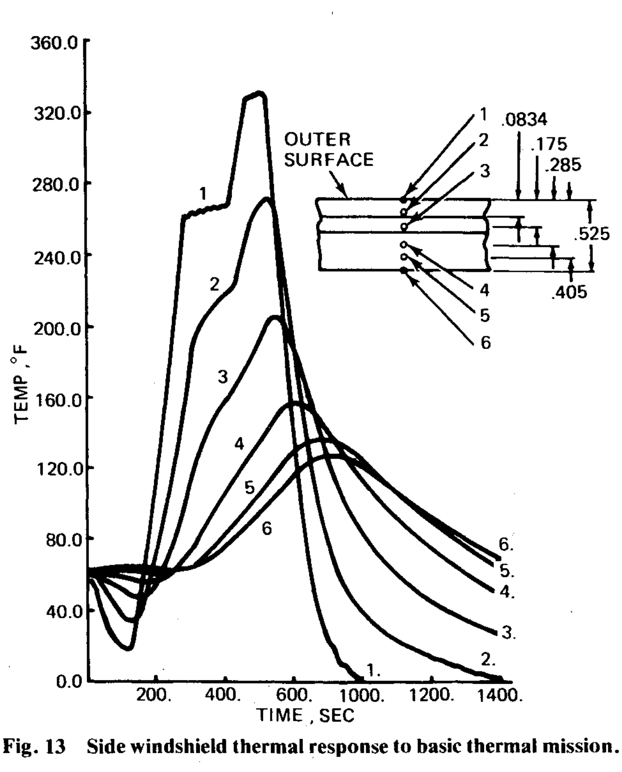

Fig. 13 Side windshield thermal response to basic thermal mission.

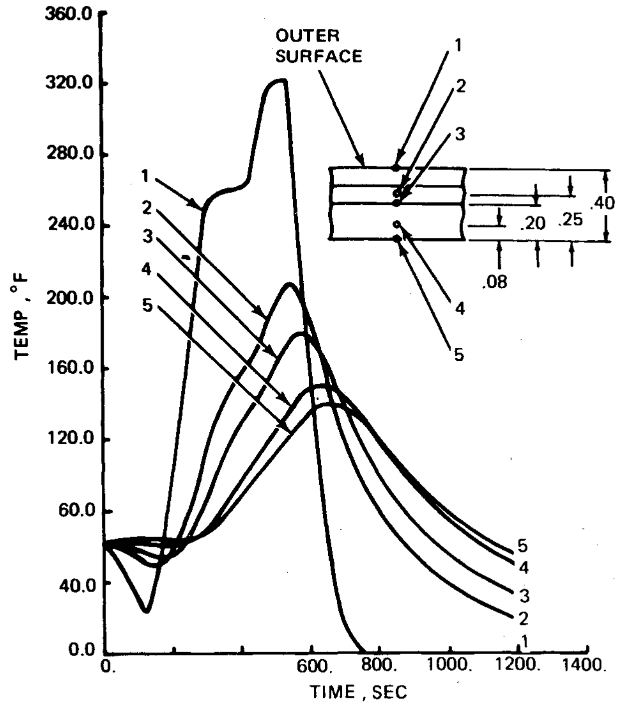

Fig. 14 Forward canopy thermal response to basic thermal mission.

breakdown. As expected, the backface temperature is not greatly affected by the aerodynamic heating, and changes slowly from its initial value resulting in a considerable thermal gradient across the windshield (because of the thick cross section). The side windshields were analyzed as a 0.525-in.-thick trilaminate built up as shown in Fig. 2. A temperature/time history for the side windshield subjected to the Thermal Mission Profile is presented in Fig. 13. The temperature distribution reveals that the load-carrying stretched acrylic never reaches a temperature above 180°F throughout the entire mission. The forward canopy crease thermal response is shown in Fig. 14. It may be observed that the trilaminate construction of the forward canopy provides sufficient thermal protection to arrest a 185°F temperature penetration to the load-carrying laminate under the worst thermal conditions. This is sufficiently below 220°F (above which significant thermal relaxation of stretched acrylic takes place).

The rear canopy leading-edge temperature response curve is shown in Fig. 15. Compare the maximum temperatures of the inner structural ply with those shown in Fig. 9 for the monolithic rear canopy. (Note the significant reduction in temperature due to the trilaminate concept.)

Thermal Stress Distribution

Front Windshield

The windshield and canopy thermal stress distributions were obtained on an F-14-developed thermal stress program.[7] The program can compute thermal stress distributions in thin or thick multimaterial composites with temperature-dependent properties. A multiplicity of boundary conditions may be specified.

The front windshield thermal gradients (Fig. 12) were used as the basis for analysis. Thermal stress distributions through the windshield were obtained at several mission time slices in search of critical conditions. Maximum tensile stresses on the inner ply occur at 528 sec into the mission. Stress distribution through the windshield is shown in Fig. 16. The thermal stresses shown are considered to be conservative because of the conservative fixity assumptions made in the analysis. The thermal stresses were combined with the stresses resulting

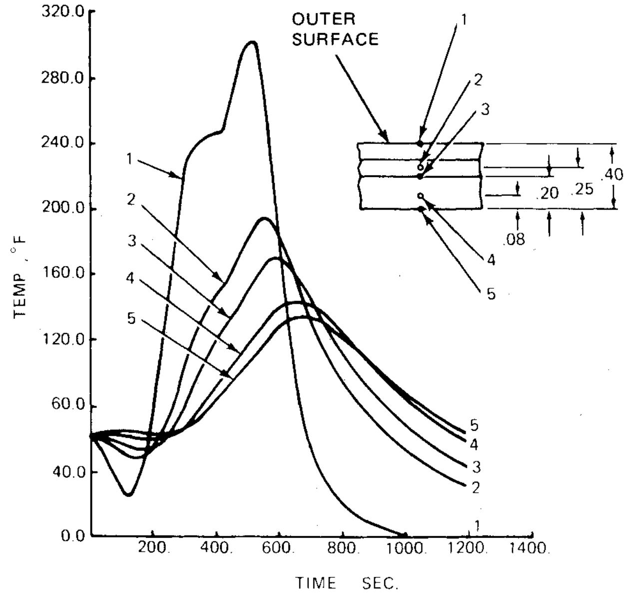

Fig. 15 Rear canopy thermal response to basic thermal mission.

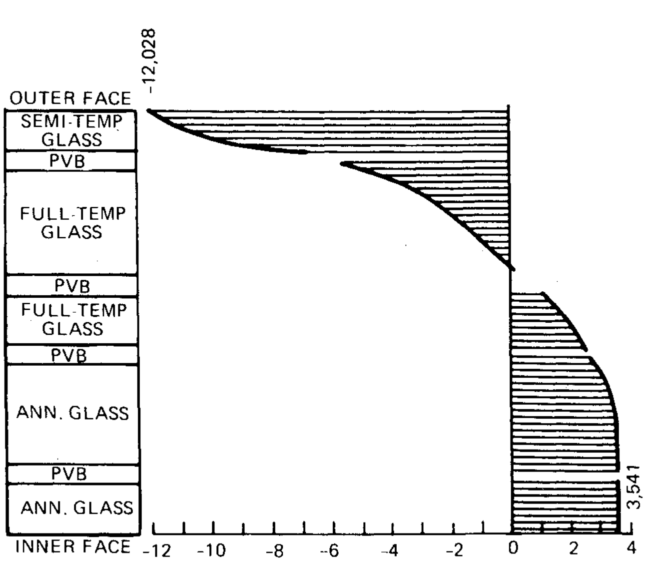

Fig. 16 Front windshield thermal stress distribution, $\theta = 528$ sec.

from the external aerodynamic and internal pressurization loads to obtain the total windshield stress distribution (Ref. 2).

Forward Canopy

A similar analysis was conducted on the forward canopy. In the case of the canopy the analysis was done for the existing F-14 acrylic transparency as well as on an equivalent polycarbonate transparency. The purpose of the analysis was to obtain a comparison of the thermal stress distributions in the two systems. The polycarbonate configuration analyzed was a monolithic 0.30-in.-thick sheet of Lexan SL-2000.

The stresses shown in Fig. 17 were obtained by maximizing the acrylic thermal stress distributions obtained at several times slices of the thermal gradients (Fig. 14). Maximum tensile stresses (937 psi) in the acrylic system occur at 420 sec into the mission. The corresponding stresses in the polycarbonate are also shown, as well as configurations for the two systems. (The thermal gradients for the polycarbonate are not shown in this paper.)

The maximum thermal stress in the polycarbonate (not shown here) is 1284-psi tension, and it occurs at 570 sec into the mission. All stresses were calculated on the assumption that the canopy behaves as a thick cylindrical shell, fully restrained in bending, and unrestrained in axial expansion. Edge effects were not included in the analysis. The thermal stresses in the acrylic transparency were combined with the stresses resulting from the aerodynamic and pressurization loads to obtain the total canopy stress distribution. This is shown in more detail in Ref. 2.

In comparing the thermal stress distributions obtained on the acrylic and on the polycarbonate canopy, it was found that the compressive stresses on the polycarbonate outer surface are two to five times the stress on the outer surface of the stretched acrylic. It was also found that the inner surface of the polycarbonate is subjected to tensile stresses that are three times larger than the corresponding stresses on the stretched acrylic. This occurred at a point in the mission profile where the temperature is the highest.

Canopy Distortions in Extreme Thermal Environments

In-service experience on the F-14 aircraft indicated that extremes in the ambient environment influenced the canopy lock and unlock functions. Canopy closure problems were encountered when the outside ambient temperature went below 20°F (approximately), or exceeded 95°F (approximately). Canopy thermal distortions were identified as the cause of the closure malfunction.

An analysis was conducted to determine if the use of polycarbonate glazing materials would alleviate the thermal

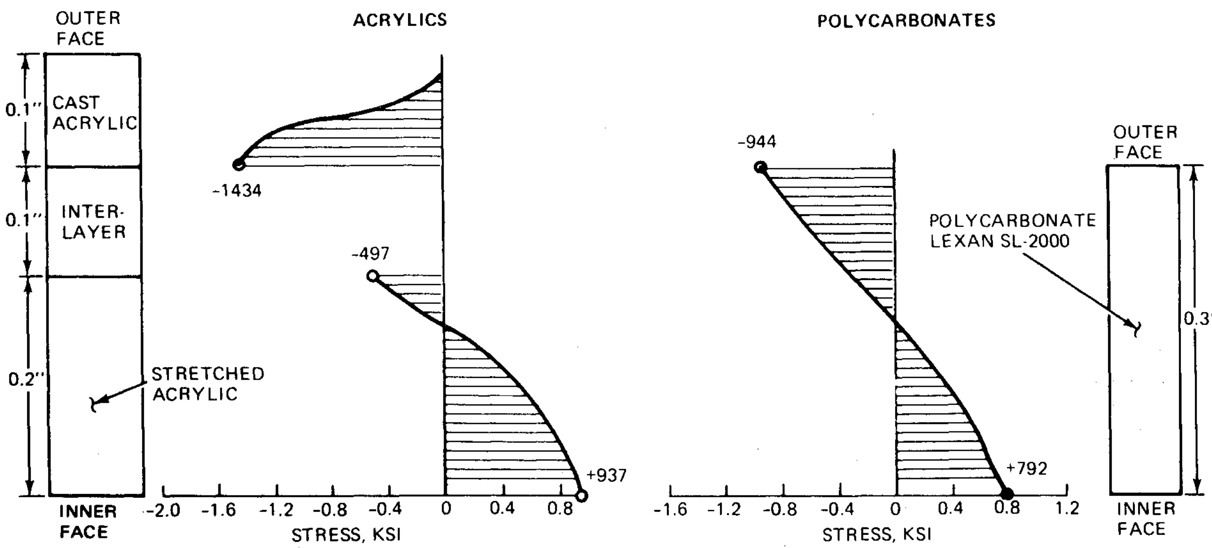

Fig. 17 Forward canopy thermal stress distribution, $\theta = 420$ sec.

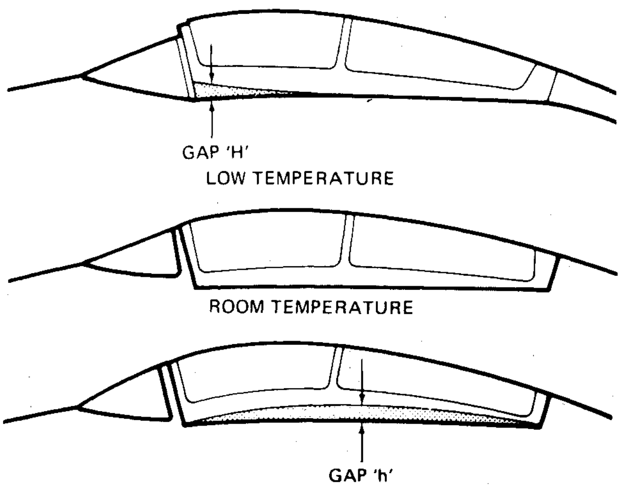

Fig. 18 Canopy thermal distortion.

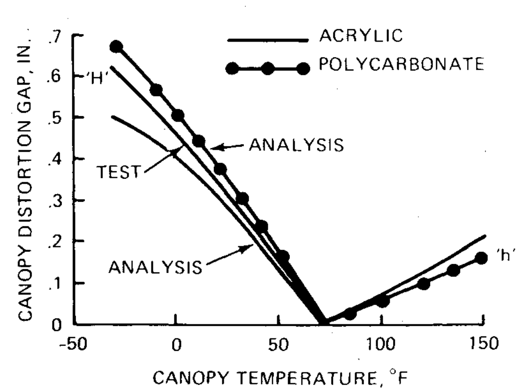

Fig. 19 Canopy distortion vs temperature for acrylics and polycarbonates.

distortion problem. The bimaterial (aluminum frame plus acrylics) canopy construction caused the canopy to distort differently when unlocked in low- and in high-temperature environments, producing the gaps indicated in Fig. 18. The object of the analysis was to determine the magnitude of the gaps H and h for acrylics and polycarbonates at various temperatures.

Results of the analysis are shown in Fig. 19, where the distortion gaps H and h are plotted as a function of temperature. Also shown are the test data obtained with the present acrylic canopy. It may be observed that a polycarbonate canopy will distort more than the present acrylic canopy at low temperatures, and slightly less at high temperatures. At −30°F, for example, the polycarbonate canopy will distort 0.676 in., compared to 0.503 in. for an acrylic canopy. At 140°F the distortion gaps are 0.140 in. for polycarbonates and 0.179 in. for acrylics. It was concluded that replacing the present canopy with a polycarbonate canopy will not solve the canopy distortion problem.

A series of tests was conducted in which the thermal distortion characteristics of the existing canopy and the operating thermal envelope of the canopy lock/unlock system was established. Several modifications to the canopy/cockpit locking hooks, and an increase in the canopy locking cylinder pressure, have solved the canopy closure problem. The tests showed that in a sled test incorporating the above changes, a production F-14 canopy could be fully locked and unlocked between the temperature extremes of −65 to +160°F. Details of the performed tests are given in Ref. 8.

Predicted vs Measured Canopy Temperatures

The F-14 canopy was engineered and designed to perform safely throughout the entire flight envelope at all operating

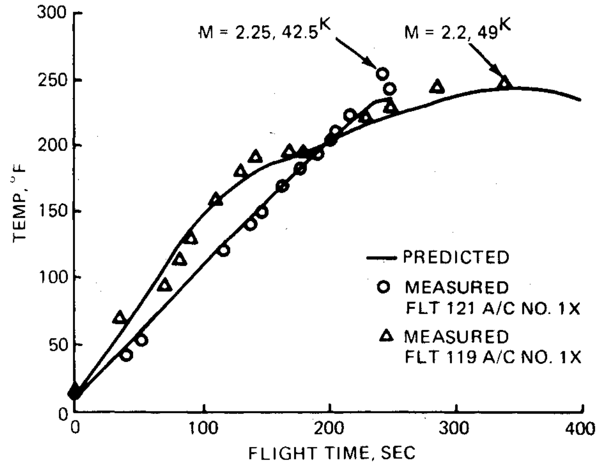

Fig. 20 Predicted vs measured outer surface canopy temperatures.

and loading conditions. Of particular interest, however, is its performance at the Mach 2+ design point for which it was optimized. To compare canopy-predicted temperatures with in-flight measured temperatures, two high-speed flights on aircraft No. 1X (Flights 119 and 121) were chosen for correlation.

A comparison between the predicted and measured canopy outer surface temperatures for the two flights is shown in Fig. 20. The comparison was made for the forward canopy leading edge. As can be seen from the data, the correlation is fairly good.

Conclusions

The F-14 transparency design can be called a success when all constraints under which it was conceived and implemented are considered. This was borne out by six years of near failureless operation, from first flight through carrier deployment. This conclusion has been further reinforced by the transparency problems encountered on several current combat aircraft. In some, several basic redesigns were implemented; in others, configurational and/or material changes are being considered seriously.

Acknowledgment

The author acknowledges with appreciation the assistance of D. Riddle, E. Cohen, and J. Myles, from Grumman Aerospace Corp.; W. Pick and V. Brand, from Swedlow; and S. Davis and W. Fischer, from PPG.

References

[1]Doucette, A.R., "The F-14 Aircraft Head-Up Display," *Proceedings of the IEEE National Aerospace and Electronics Conference*, Dayton, Ohio, June 12, 1975.

[2]Cohen, E., Johnson, S., and Cyphers, R., "Stress and Fatigue Analysis of F-14 Fuselage Forward Module," Grumman Aerospace Corp.,Bethpage, N.Y., A51-313-R-08.211, March 1971.

[3]Mott, M.J., "Experimental Investigation into the Bird Impact Resistance of Flat Windscreen Panels with Clamped Edges," Air Force Materials Laboratory, Wright Patterson AFB, Ohio, AFML-TR-73-126, June 1973.

[4]Przemieniecki, J.S., "Design of Transparencies," *Journal of the Royal Aeronautical Society*, Vol. 63, Nov. 1959, pp. 620-636.

[5]Cannizzaro, C., "Heat Transfer Coefficients and Boundary Layer Temperature Along the F-14 Canopy," Grumman Aerospace Corp., Bethpage, N.Y., A51-336-I-69-5, May 15, 1969.

[6]Kelley, G., "VFX Canopy Aero-Heating Estimates," Grumman Aerospace Corp., Bethpage, N.Y., IOM-69-22, April 3, 1969.

[7]Fixler, S.Z., "Computer Program To Calculate Thermal Stress and Deformation in Structures," Grumman Aerospace Corp., Bethpage, N.Y., A51-313-I-74-2, Feb. 15, 1974.

[8]Kleisler, W.B., "Results of F-14A Canopy Thermal Function Test," Grumman Aerospace Corp., Bethpage, N.Y. A51-314-R-3181.11, May 6, 1974.